Journal of Physics: Conference Series

DIC technique for experimental validation of higher order numerical models

DIC technique for experimental validation of higher order numerical models

Nandini Priya Thatikonda, Daniele Baraldi, Giosuè Boscato and Antonella Cecchi

IUAV University of Venice, Santa Croce 191, Venice 30135 - Italy.

E-mail: npthatikonda@iuav.it, Orcid ID: 0000-0001-7503-7340

Abstract.

This paper presents an adaptation to the Digital Image Correlation (DIC) technique to aid and improve standard measurement methods in experimental mechanics. The practical application is demonstrated by the validation of the Cosserat Continuum model, using small-scale masonry specimens. Numerical models, such as the Cosserat continuum, play an important role in the identification and description of the mechanical behaviour of structures. Especially when it comes to anisotropic and quasi-brittle materials like masonry, these models are needed to evaluate significant aspects like performance, safety, or the effects of various strengthening interventions. The experimental investigation to validate a numerical model is not always straightforward and several of them remain theoretical. Addressing this, the experimentation presented in this paper evaluates the Cosserat identification in shear, where along with simple shear deformation, rigid rotations, micro rotations and micro couples are also exhibited. With such complex deformations, conventional techniques, such as strain gauges, or extensometers can no longer be adopted. The adapted DIC allows the quantification of these deformation data and validates the numerical model.

1. Introduction

In the fields of solid mechanics and material sciences, the accurate measurement and analysis of displacements, deformations, strains, and changing shapes are fundamental in comprehending the behaviour and mechanical characteristics of various materials, composites, or structures. While conventional methods, such as strain gauges and extensometers, have provided valuable insights into simpler problems, when complexity in deformations is presented, their applicability becomes limited.

Within this context, optical techniques and vision-based methods have emerged as an alternative to point-wise strain gauge techniques, to allow for capturing complex measurements. Amongst several of these techniques, over the last decades, Digital Image Correlation (DIC) has gained popularity, due to its versatility, efficiency, accuracy and applicability across a wide range of scales, specimens and environments.

DIC is a non-contact technique developed in the early 1980s, aimed at the measurement of changing shape, deformations, and strains of an object [1]. For its application in experimental mechanics, a series of digital images of the specimen are captured under several loading conditions. Through the correlation between these images before and after deformations, full-field deformation, strain or motion data could be extracted and analyzed. The correlation is

based on tracking the movement of small image subsets between reference and deformed image and is extended over the entire image to create a grid of displacement vectors, which provides full-field information.

While 2D-DIC emerged as the foundational method, enabling the assessment of planar deformations, the literature also presents several other adaptations and applications for a wide range of data capturing [2]. The need for simultaneous perspectives of measurement, comprehensive three-dimensional insights and to provide multiple viewpoints to analyze complex deformations derives from methods such as 3D-DIC, multi camera-DIC and stereo DIC [3]. Recent advances in the multi-viewpoint approach, coupled with the development of precise interpolation algorithms, have led to the introduction of techniques like Digital Volume Correlation (DVC) [4], which could present a consolidated application for all out-of-plane deformations. Further, the advancement of high-speed cameras in recent years has prompted researchers to explore advanced techniques like high-speed imagining DIC and video-aided DIC [5], which are suited for analyzing fast or dynamic events characterized by small displacement and temporal amplitudes [6–8]. The literature also presents several innovative applications of DIC-based technology for non-destructive evaluations and structural health monitoring [9; 10].

DIC applied in the context of masonry provides valuable insights by evaluating full-field strain distributions, localizing failure zones, and identifying different deformation mechanisms. In fact, it is widely adopted to assess crack development and propagation and further help in optimizing reinforcement strategies for enhancing the performance and safety of masonry structures [11–14].

Several studies have proven DIC's effectiveness and versatility, with innovation in its application to solve several problems, however, some challenges are also presented. Common early-stage issues are encountered in surface or specimen preparation, computational demands, and assumptions about the material response, but could be effectively managed with repetition and experience [1]. On the other hand, aspects such as selecting appropriate subsets, dealing with noisy environments, and addressing strain discontinuities caused by poor correlation between images or even neighbouring subsets are considered significant hurdles as they directly impact the accuracy and reliability of the results [1; 15].

Further, DIC's development is centred around correlation algorithms and has found widespread applications in the experimentation of homogeneous materials or surfaces where speckle patterns can be effectively introduced [11; 16]. When it comes to masonry structures, their inherent texture and heterogeneous nature pose unique challenges. The difficulties in obtaining a clear, discrete and consistent speckle pattern on masonry surfaces and the variations in scale across masonry specimens with respect to the speckle scale and image resolution, could potentially lead to errors while tracking the deformations or may need simplifications and large approximations. Often researchers have encountered highly inaccurate outcomes, and noise in the data due to insufficient pixel sizes, and have tried to address this by reducing the field of view, instead of capturing entire specimens [11; 13].

Furthermore, DIC is typically employed to analyze full-field deformations, and local strains and track crack propagation, yet, in experimental mechanics, their quantification and direct comparison with global loads or stresses are not always straightforward. Literature also presents hybrid approaches, where DIC adopted for masonry is often used in conjunction with traditional techniques such as strain gauges and transducers and a comparison of point-wise strain data is made to assess its accuracy and suitability [11; 14]. These simplified strain measurements, though practical in several cases, primarily stem from theories involving significant approximations, that aim at deriving global structural behaviour, simplifying the complexities of the materials involved, i.e., aspects such as heterogeneity, geometry and texture in the case of masonry.

Masonry has been the subject of extensive research over the last few decades, with several numerical models proposed across various scales, ranging from the macro models to the micro-mechanical scales. Within this multifaceted landscape of masonry analysis, several micro-

modelling approaches have been proposed, which have proven instrumental in providing insights into masonry's constituent-level or local failure mechanisms and allowing for more realistic simulations. Amongst these is the Cosserat continuum model, which offers a distinctive advantage over other models, in retaining crucial geometric information about the media it represents, enabling the identification and analysis of a wide range of deformations and strains. Further, the model facilitates the segregation of symmetric and skew components, particularly in shear, which forms a significant feature in the context of composite materials like masonry. The theoretical background and literature on Cosserat models applied to periodic brickwork like masonry is well established [17–20]. While this application of the Cosserat model to characterize masonry is fairly recent, several studies also present its extensive application in a broader domain with intricate geometries, such as hexagonal media with skewed or concave unit forms, lattice structures and other void matrix systems [21–23].

Masonry mechanical characterization, however, not only relies on theoretical modelling but also encompasses an experimental component. Experimental investigations span various scales, from simulating entire structural elements to testing panels representative of composite materials and further to the characterization of individual elements i.e., brick units and mortars [24]. The focus of this research is the shear characterization of masonry, an area that presents unique challenges, due to the quasi-brittle nature of masonry, the scale of testing, and the complexities of boundary conditions. As recommended by standards and guidelines [25; 26], large-scale specimens are commonly employed for assessing this global behaviour of masonry. However, these large-scale tests face challenges inherent to their size and the brittleness of the masonry composite itself. While failure in masonry is typically localized, the objective of these tests is to quantify global behaviours, including the impact of reinforcement in strengthened specimens [27; 28].

The coexistence of both symmetric and skew components in the Cosserat identification model implies that the deformations presented will not be straightforward and must be carefully assessed. Given these considerations, the current research aims at a simplistic adaptation of the DIC techniques, primarily to extract and quantify the Cosserat shear deformations presented in small specimen scales and further validate the numerical predictions.

The following section 2 focuses on the adaptation of the DIC technique, and how it is tailored based on periodic heterogeneous media. Section 3 gives a brief outline of the Cosserat continuum model, that will later be validated. The experimental realization, with choice of specimen, test setup, and importantly the data acquisition with DIC is presented in section 4. The experimental outcomes and a comparison with numerical data is briefly discussed in section 5, followed by the conclusion in section 6.

2. Adaption of the DIC technique

The correlation algorithms employed in the DIC technique operate by tracking the positions of a subset of pixels. The subset's positional data from before and after deformation, along with information on the positions of its neighbouring subsets is used to extrapolate and estimate full-field deformations. For this, a stochastic intensity pattern or speckle pattern, either fabricated or using the natural texture of a specimen, is adopted. Using the high contrast features of this pattern with varying grey-scale intensity, discrete subsets are created and accessed [1]. While there are certain challenges in this method, the correlation algorithms prove to be highly effective in scenarios involving deformable homogeneous materials, characterized by relatively continuous deformations. However, as previously highlighted, significant challenges are presented when applied to non-homogeneous materials and complexities in deformations, such as brittle fractures, wide cracks, and variations in the surface. Examples of poor correlation and errors in interpolation in such cases are also presented in the literature [13; 14].

To tackle the issue posed by non-homogeneous materials, such as masonry, an adaptation to

the DIC technique with a shift from speckle to tracker or marker-based methods is proposed. Here, rather than aiming at calculating full-field data, strategically selected points on the specimen surface (see figure 2) and its environment are tracked. These points are equipped with high-contrast markers or targets, and their movement through the images is extracted.

The adaptation stems from the understanding of the response of the material tested, and the kind of deformations that are anticipated. In the current case of masonry, due to significantly stiffer brick units, the deformations and failures are assumed to be localized at the mortar joints. The measure of the deformation of the composite could be assessed as the jump in displacement between two blocks and can be captured as: $\Delta u_{\perp} = u_{i,i}$ the displacement perpendicular to the axis of the mortar joint (figure 1a), $\Delta u_{\parallel} = u_{i,j}$ the displacement parallel to the joint (figure 1b) and ω_3 relative rotation between them (figure 1c).

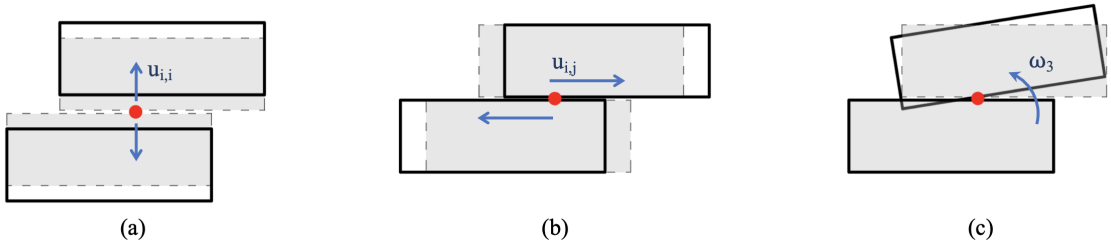

Figure 1. Deformations derived from the relative motion of two interacting blocks

A minimized tracking for a block's movement can be achieved by focusing solely on monitoring its center, which efficiently captures $\Delta u_{\perp}$ and $\Delta u_{\parallel}$ translations. However, to accurately compute the rotation, a more comprehensive reference beyond the block center is needed. A line defined by two markers positioned on the block is introduced, as shown in figure 2. This approach not only tracks relative movements between blocks but also has the capability to detect and quantify any internal deformations, although, in the current case of traditional masonry, this may not be critical, given that the blocks are generally much stiffer than the joints.

An open-source DIC algorithm, as developed by [29], is employed, and the correlation code is adapted to specifically track the chosen points. This adaptation involves tracing the movement of the markers between their undeformed and deformed states. Furthermore, a MATLAB code was developed to calculate absolute displacement, absolute strain, as well as relative and internal strains, which will be applied in this study.

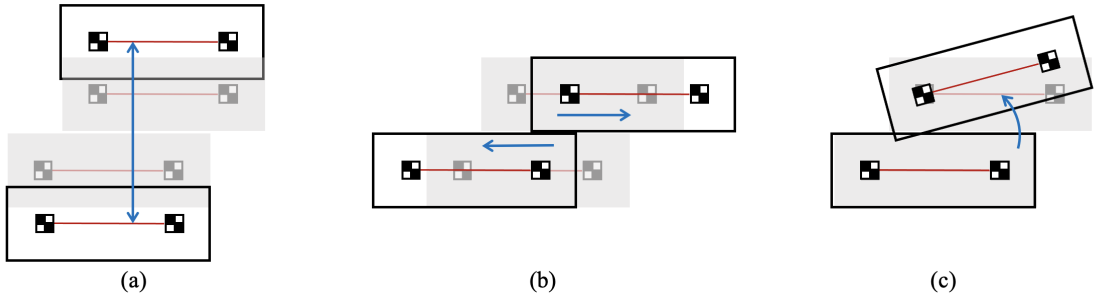

Figure 2. Point wise marker scheme for tracking the relative motion of the blocks

This shift towards point-wise tracking introduces a level of granularity that enables the measurement of strains between individual points, offering numerous direct and indirect measurement possibilities. In cases where the material exhibits abrupt changes or discontinuities, these markers continue to maintain their reference characteristics, making them ideal for tracking purposes.

One of the notable advantages of this adapted DIC approach is its flexibility in accommodating variations in specimen scale. As the distance between the camera and the specimen, along with the desired image resolution, can vary significantly, this adaptation allows for easy customization. Researchers can adjust the camera's position and image resolution to cover specific parts or the entire specimen as required, ensuring optimal data acquisition in varying scenarios, and tailoring the methodology to their specific requirements. This customization capability enhances the versatility of DIC, making it applicable to a wide range of material scales and structural complexities.

3. The Cosserat Continuum model

The representation of periodic masonry as a 2D Cosserat media is adopted from literature presented in [17; 19]. Here masonry is represented as a composition of rigid blocks, interacting with elastic mortar joints. The deformation of the interfaces is given as a function of the traction due to the relative displacement of the blocks and is defined by its normal stiffness K' and shear stiffness K''. Following the notation presented in [30; 31], the stress tensors $\boldsymbol{\sigma}$ and $\boldsymbol{\mu}$ could be defined, where, the former collects the in-plane stresses, and the latter accounts for micro couples. The constitutive law defining the stress-stain relations can be given as:

$$\sigma_{ij} = A_{ijkl}\varepsilon_{kl} \quad \mu_{i,3} = L_{i3}\chi_{3,i} \tag{1}$$

where, A_{ijkl} collects the homogenized Cosserat elastic linear and shear coefficients, and $L_{i,3}$ presents the homogenized flexural coefficients associated with the curvatures, for $i, j, k, l = 1, 2$.

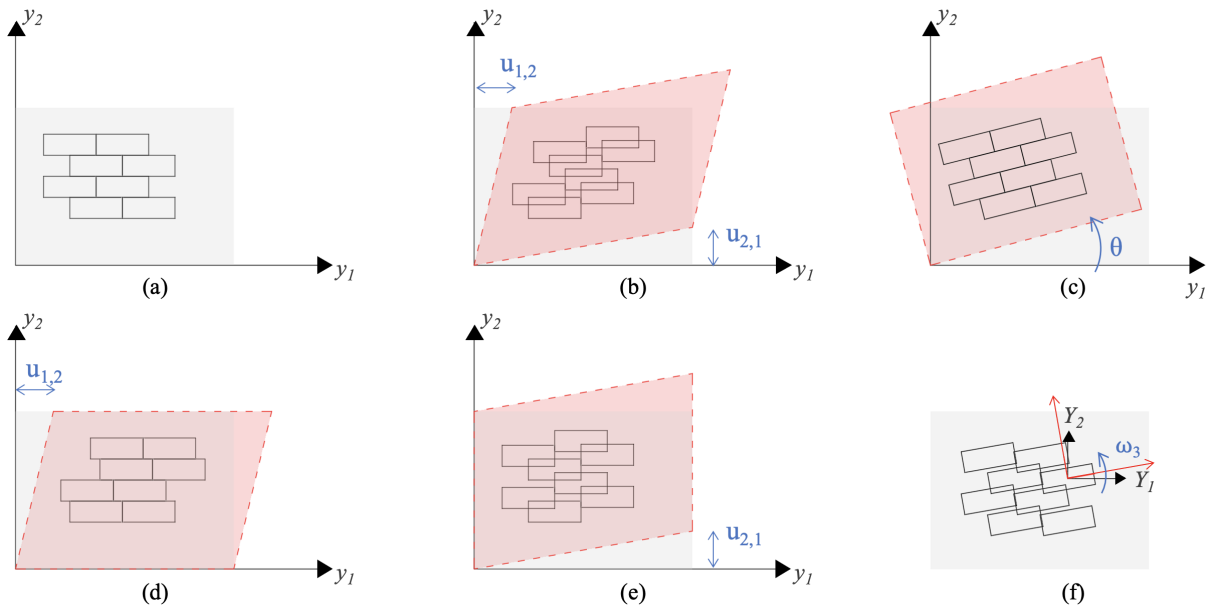

Figure 3. Deformation configurations of a continua (a) Undeformed media with the global reference axis y_1, y_2, (b) Cauchy total shear, (c) Rigid rotation, (d) Partial shear about y_1 direction, (e) Partial shear about y_2 direction and (f) Micro rotation about the local axis Y_1, Y_2

The characteristic efficiency of the Cosserat model, different from the classical Cauchy continuum can be clearly identified in the strain tensor ε_{ij}. The definition of shear in a Cauchy media is given as a unified total shear deformation ε^c_{12}, as shown in figure 3b, whereas, the Cosserat model presents an orthotropic representation of shear [19; 32; 33], accounting for the

additional rotational degree of freedom, ω_3 (see figure 3f) with two pure shear deformation states ε_{12} and ε_{21}. These shear strains are given as,

$$\varepsilon^c_{12} = \frac{u_{1,2} + u_{2,1}}{2} \qquad \varepsilon_{12} = u_{1,2} + \omega_3 \qquad \varepsilon_{21} = u_{2,1} - \omega_3 \tag{2}$$

where, $u_{1,2} = \partial u_1/\partial y_2$ is the partial shear about the y_1 axis and $u_{2,1} = \partial u_2/\partial y_1$ is the partial shear about the y_2 axis, as shown in 3d and 3e, respectively.

For deriving the Cosserat coefficients, two periodic masonry textures, the running bond and the stack bond, are considered, as shown in figure 4a,c. These two textures could be considered as the limit cases defining the perfect discontinuities and continuities of the head joints in a 2D periodic masonry media. For each of these masonry typologies, the representative elementary volume or REV is defined. According to [34], a REV is a heterogeneous volume, that would contain the mechanical and geometrical information which, using an internal law of composition could reconstruct the body itself. The REV considered for the running bond and stack bond are presented in figure 4b and figure 4d respectively.

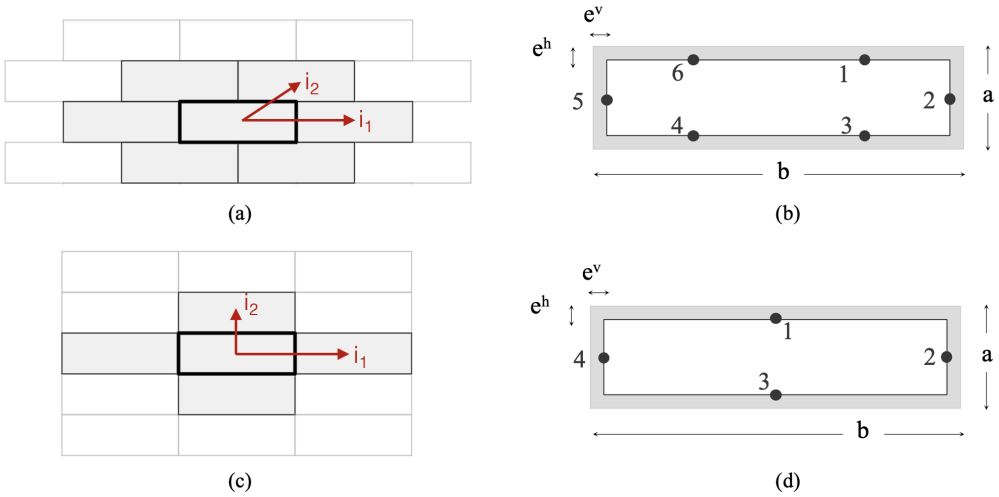

Figure 4. (a,b) REV Running bond masonry (c,d) REV Stack bond masonry

The compatible identification procedure presents a simplified representation of periodic masonry, where a uniform strain hypothesis is assumed [17; 19]. Considering this identification procedure, and an equivalence between the 2D discrete media and the 2D continua, the elastic coefficients of the Cosserat continuum, as presented in equation 1, for the running bond typology REV considered in figure 4b, are derived as follows:

$$A^R_{1111} = \frac{4K'\frac{e^h}{a} + \frac{b}{a}K''\frac{e^v}{a}}{4\frac{e^h}{a}\frac{e^v}{b}}, \quad A^R_{2222} = \frac{K'}{\frac{e^h}{a}} \quad A^R_{1212} = \frac{K''}{\frac{e^h}{a}}, \quad A^R_{2121} = \frac{4K''\frac{e^h}{a} + (\frac{b}{a})^2K'\frac{e^v}{b}}{4\frac{e^h}{a}\frac{e^v}{b}} \tag{3}$$

$$L^R_{13} = \frac{b^2}{192}\left(\frac{12K''}{\frac{e^h}{a}} + \frac{16K'}{\frac{e^v}{b}\frac{a}{b}} + \frac{4K'}{\frac{e^h}{a}\frac{a}{b}}\right), \quad L^R_{23} = \frac{K''a^3}{4e^h} + \frac{K'ab^2}{12e^h} \tag{4}$$

Similarly the components of the Cosserat elastic tensors A_{ijkl} and L_{i3} for the stack bond typology REV considered in figure 4d, are derived as:

$$A^S_{1111} = \frac{K'}{\frac{e^v}{b}}, \quad A^S_{2222} = \frac{K'}{\frac{e^h}{a}}, \quad A^S_{1212} = \frac{K''}{\frac{e^h}{a}}, \quad A^S_{2121} = \frac{K''}{\frac{e^v}{b}}, \tag{5}$$

$$L_{13}^{S} = K'' \frac{b^3}{4e^v} + K' \left(\frac{a^2 b}{12e^v} + \frac{b^4}{ae^h} \right), \quad L_{23}^{S} = K'' \frac{a^3}{4e^h} + K' \left(\frac{b^2 a}{12e^h} + \frac{a^4}{be^v} \right) \tag{6}$$

The Cosserat continuum model serves as the theoretical foundation for analyzing various deformations presented in masonry. However, the current research focuses on the A_{1212} and A_{2121} in-plane shear deformations. The subsequent sections will focus on the practical aspects of our study, including specimen selection and the experimental setup, which are crucial for validating the Cosserat model's predictions, effectively bridging theory with the experimental.

4. Experimental realization of the continuum model

The experimental realization of the numerical model involves three key components: the choice of specimens, the design and configuration of the test setup, and data acquisition and processing of the outcomes. These crucial steps collectively facilitate the derivation of elastic coefficients and help define the mechanical characteristics under investigation.

4.1. Choice of specimen

The specimens for the experiments proposed are derived from two masonry textures, the running bond and the stack bond. The running bond masonry typology presents a diagonal composition of joints, with perfect discontinuities in the head joints, whereas the stack bond masonry typology presents continuous head and bed joints. The choice of these two textures allows for evaluating the limit cases in periodic masonry, with continuous mortar joints vulnerable to shear failure, and discontinuity that participates in and facilitates shear resistance.

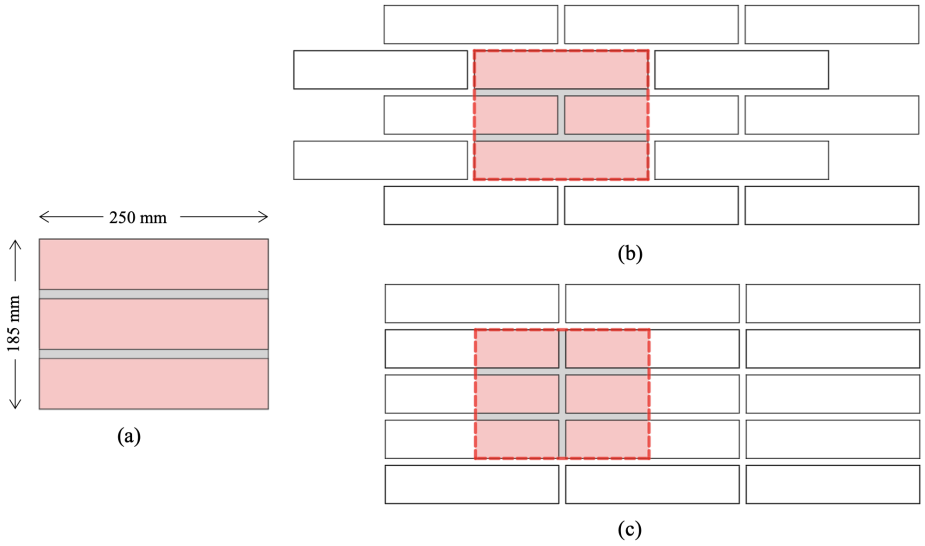

Figure 5. (a) The standard triplet specimen (b) Running bond masonry, with the modified running bond triplet proposed (c) Stack bond masonry, with the modified stack bond triplet proposed

To practically realize these masonry textures, the standard masonry triplet specimen was adopted from the standards EN-1052-3 [35] (as figure 5a) and two modifications to this specimen were proposed: an introduction of one head joint in the second course and an introduction of a continuous head joint through all three courses to represent running and stack bond textures respectively.

The specimens were made of solid clay bricks and lime mortar joints. The bricks were $230\times110\times55mm^3$ in size, with a density of $1710kg/m^3$ and a compressive strength of $10.63MPa$, computed according to the standard EN 772-1 [36]. The lime mortar used to make the masonry joints contained mainly natural hydraulic lime, aggregates, and additives, with a compressive strength of $1.4MPa$, with a coefficient of variation of 3.3%, computed according to the standard EN 1015-11-1999 [37]. Additionally, the lime mortar elastic modulus (E_m) of $127.89MPa$ was derived from the tangential slope of the stress-strain curves recorded for the specimens in compression.

4.2. Test setup

For the practical realization of the shear tests, a frame was designed as shown in figure 6. The force was applied horizontally at frame (3), and pure shear deformation was introduced with the help of two members, (4) and (5) that are in contact with the specimen. Here, member (5) transfers the load to the specimen and (4) acts as a fixed support. In the first setup, the specimen was placed horizontally, and a force was applied parallel to the bed joints (see figure 6a,b), simulating horizontal shear deformation (ε_{12}). In the second setup, the specimen was rotated by 90 degrees to the vertical position, and force was applied perpendicular to the bed joints (see figure 6c,d), simulating vertical shear deformation (ε_{21}).

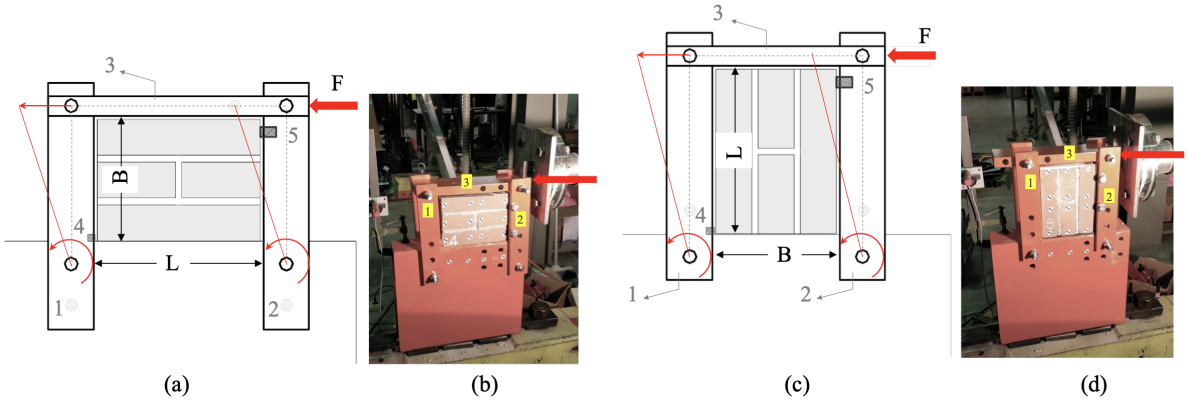

Figure 6. (a,b) Horizontal testing configuration proposed (c,d) Vertical testing configuration proposed

4.3. Data acquisition and processing

With the motivation to introduce pure shear deformations within the specimen, there was a provision for vertical movement of the frame (4) in both test setups. This avoided the compressive stresses due to rotation of the frames (2) and (3). This margin also accommodated the initial rigid rotation of the specimen (see figure 3c), shown in figure 7a.

The predicted pure shear deformations presented by the Cosserat identification model can be characterized by two fundamental components, as given in equation 2. The first one involves lateral sliding, signifying movement given as $u_{1,2}$ or $u_{2,1}$. The second component is the microrotation ω_3, which assumes considerable importance at this scale, see figures 7b,c,d.

The extraction of these deformations was facilitated through the utilization of the adapted DIC technique, previously introduced in section 2. The initial phase of the experimentation involved rigid rotation of the specimen with no internal strains developed. This is followed by shear deformations within the specimen were recorded, as shown in figure 7c,d.

A marker scheme was proposed taking into account the stack bond texture, involving six blocks equipped with two $15\times15mm$ size markers, see figure 8a. The same was then applied to other specimen textures to maintain consistency, as shown in figure 8b-g. Tracking the

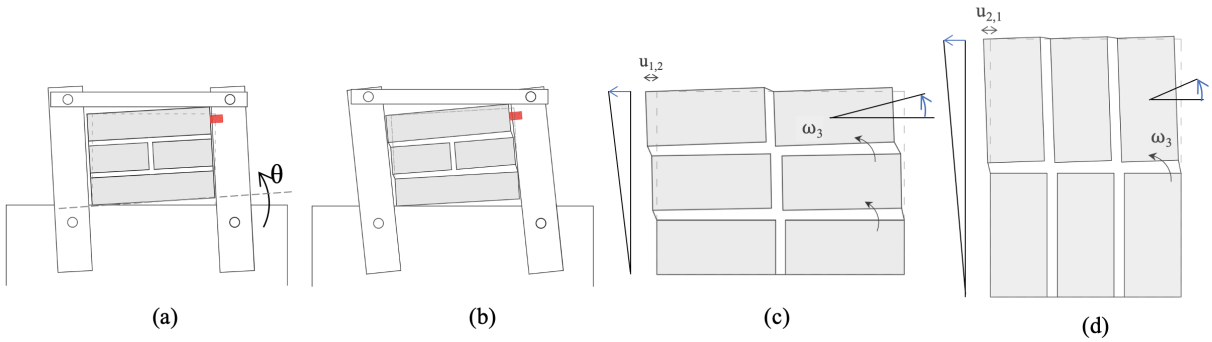

Figure 7. (a) Rigid rotation phase and (b) shear deformation phase of the specimen, (c, d) the predicted shear deformations illustrated for stack bond specimen (in horizontal and vertical testing configurations)

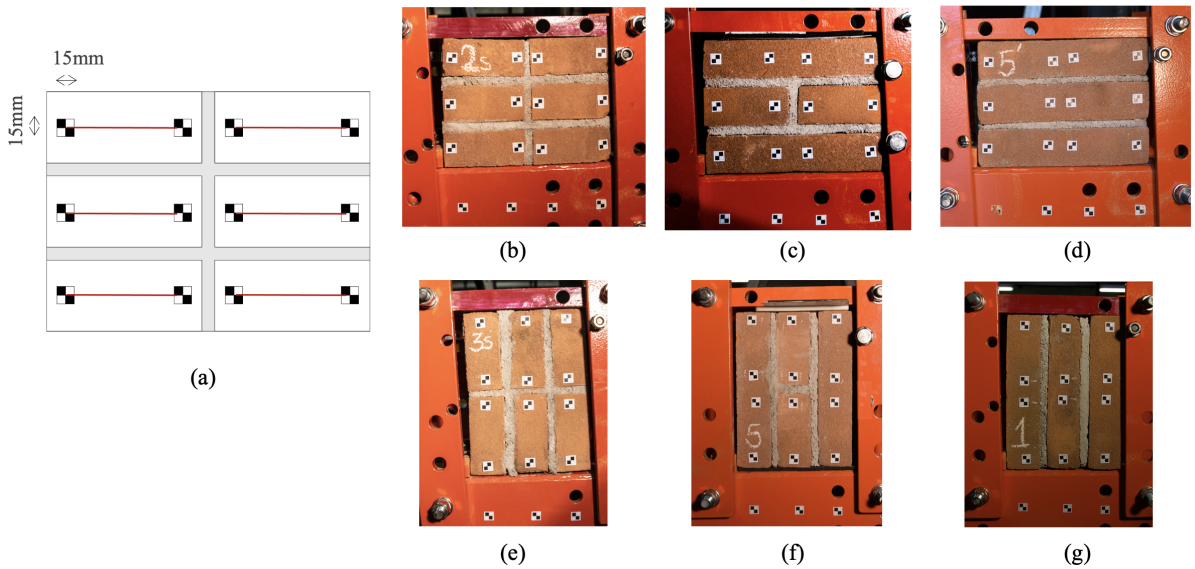

Figure 8. DIC marker scheme applied for the different specimen typologies

displacements of these markers, the relative block displacements, micro-deformations $u_{1,2}$, $u_{2,1}$ and ω_3 were captured, and the initial rotation was filtered out.

5. Experimental Outcomes and validation of the Numerical model

In this study, along with both the modified triplet typologies, the standard triplet specimens was also considered to be tested in shear. A total of 18 specimens were tested, three of each texture, tested under the two shear configurations previously defined in figure 6. The applied forces were recorded by the actuator, and the shear deformations according to equation 2 were extracted from DIC. These test results, after filtering out the initial rotation, are presented as stress-strain plots in figures 9 and 10. It can be noted that similar shear behaviour was observed across different masonry textures in the horizontal configuration, likely due to the presence of continuous bed joints having a consistent response to horizontal shear. In contrast, the vertical configuration shows distinctions among the adopted textures. The presence of a continuous head

joint in the stack bond triplets encourages joint interaction and the involvement of both head and bed joints. However, standard triplets and running bond triplets demonstrate sliding failure at the interfaces between the joints and bricks.

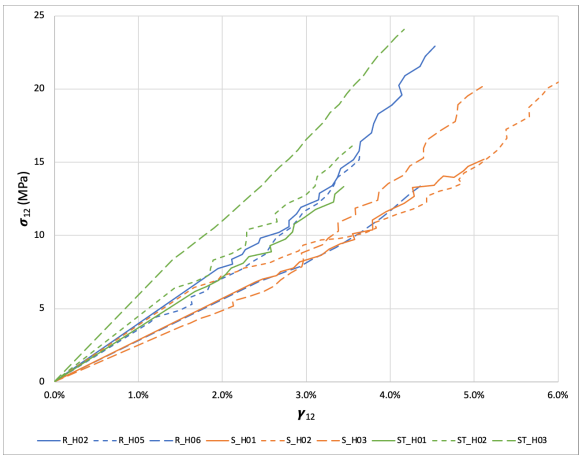

Figure 9. Stress strain plots for specimens tested in Horizontal Configuration

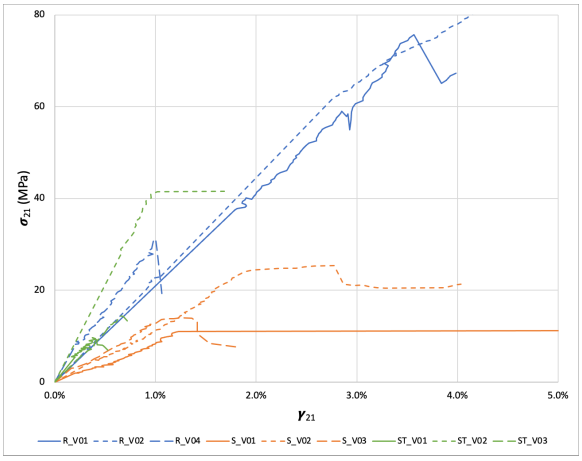

Figure 10. Stress strain plots for specimens tested in Vertical Configuration

For the validation of the numerical model, the running and stack bond textures are considered. The stiffness ratio of brick to mortar ($E_b/E_m = 32.9$) is significantly high, supporting the hypothesis of stiff blocks and weak mortar, of the Cosserat model. Considering the mechanical parameters of the constituent materials and assuming a standard Poisson's ratio of $\upsilon_m = 0.2$, the components of the interface stiffness tensor can be computed as $K' = 13.5N/mm^3$ and $K'' = 5.4N/mm^3$ (computed according to [19; 30]).

Table 1. Shear stiffness coefficients for the Cosserat continua computed from equations 3 and 5, compared with the experimental values

	A_{1212} (MPa) Cosserat	Experimental	A_{2121} (MPa) Cosserat	Experimental
Running bond masonry	346	363.84	4849	2454.40
Stack bond masonry	346	324.52	1384	1095.24

This derived stiffness tensor, along with the geometrical information of the specimen is considered to compute the A_{1212} and A_{2121} coefficients of the Cosserat micropolar model as given by equations 3 and 5, is presented in table 1. Further, to validate the Cosserat continuum model, a comparison is established between the experimental stiffnesses, by considering a mean of the three specimens tested for each of the masonry textures, also tabulated in table 1.

Summarizing the findings, the Cosserat model predicts consistent horizontal shear stiffness (A_{1212}) for both running and stack bond specimens in the horizontal configuration, aligning well with experimental results. In the vertical configuration, the model indicates significantly higher stiffness (A_{2121}) for running bond specimens compared to experimental data, while the stack bond specimens' stiffness is higher but remains within the range of experimental outcomes. This could be attributed to two factors, firstly, the geometrical variation between the specimens and the REV considered in the numerical model and secondly to the type of failure observed.

6. Conclusion

This paper presents an adaptation of the Digital Image Correlation (DIC) technique, demonstrating its potential to aid measurements in experimental mechanics. The validation of the Cosserat continuum identification model explores the segregation of complex and coexisting deformations and strains. DIC addresses the gap in recording such data, where conventional techniques can no longer capture the complexities involved. The knowledge of the deformation and deriving simplified marker placements for DIC can help researchers use this method and explore complex problems.

Even for simpler problems, using conventional instrumentation such as strain gauges, transducers, or extensometers to record experimental data is not always cost-effective. Strain gauges are typically mono-use devices, while transducers and extensometers, though reusable, are susceptible to damage. In many cases, they must be dismounted before the specimens exhibit failure or non-linear strains, creating a significant gap in the evaluation of post-peak behaviour. Here, the proposed marker-based adaptation of DIC, and recording point-wise strains offers a cost-effective solution, without compromising in the data accuracy or quality. This economic advantage, combined with its versatility in application and to provide critical insights into complex problems, makes DIC a valuable tool for researchers across various fields.

References

[1] Sutton M A, Orteu J J and Schreier H 2009 *Image correlation for shape, motion and deformation measurements: basic concepts, theory and applications* (Springer Science & Business Media)

[2] Sutton M A, Yan J, Tiwari V, Schreier H and Orteu J J 2008 *Optics and Lasers in Engineering* **46** 746–757

[3] Solav D, Moerman K M, Jaeger A M, Genovese K and Herr H M 2018 *IEEE* **6** 30520–30535

[4] Bar-Kochba E, Toyjanova J, Andrews E, Kim K S and Franck C 2015 *Experimental Mechanics* **55** 261–274

[5] Tiwari V, Sutton M and McNeill S 2007 *Experimental mechanics* **47** 561–579

[6] Helfrick M N, Niezrecki C, Avitabile P and Schmidt T 2011 *Mechanical systems and signal processing* **25** 917–927

[7] Pierron F, Sutton M and Tiwari V 2011 *Experimental Mechanics* **51** 537–563

[8] Kalaitzakis M, Kattil S R, Vitzilaios N, Rizos D and Sutton M 2019 Dynamic structural health monitoring using a dic-enabled drone *2019 ICUAS* (IEEE) pp 321–327

[9] Jurjo D, Magluta C, Roitman N and Gonçalves P 2010 *Mechanical Systems and Signal Processing* **24** 1369–1382

[10] Niezrecki C, Baqersad J and Sabato A 2018 *Handbook of advanced non-destructive evaluation* **46**

[11] Torres B, Varona F B, Baeza F J, Bru D and Ivorra S 2020 *Sensors* **20** 2122

[12] Tekieli M, De Santis S, de Felice G, Kwiecień A and Roscini F 2017 *Composite Structures* **160** 670–688

[13] Sciuti V F, Vargas R, Guerrero N, Marante M E and Hild F 2023 *Mathematics and Mechanics of Solids*

[14] Howlader M, Masia M and Griffith M 2021 *Structures* **29** 427–445

[15] Becker T, Splitthof K, Siebert T and Kletting P 2006 Error estimations of 3d digital image correlation measurements *Speckle06: Speckles, From Grains to Flowers* vol 6341 (SPIE) pp 86–91

[16] Rajinikanth E, Aranganathan A, Vedanarayanan V, Gomathi T, Sivasundarapandian S *et al.* 2023 Strain measurement using digital image correlation technique *2023 International Conference on Advances in Computing, Communication and Applied Informatics (ACCAI)* (IEEE) pp 1–8

[17] Salerno G and de Felice G 2009 *International Journal of Solids and Structures* **46** 1251–1267

[18] Godio M, Stefanou I, Sab K, Sulem J and Sakji S 2017 *European Journal of Mechanics-A/Solids* **66** 168–192

[19] Baraldi D, Cecchi A and Tralli A 2015 *European Journal of Mechanics-A/Solids* **50** 39–58

[20] Baraldi D and Cecchi A 2018 *Computers & Structures* **207** 171–186

[21] Beveridge A J, Wheel M and Nash D 2013 *International Journal of Solids and Structures* **50** 246–255

[22] Trovalusci P and Masiani R 1999 *International Journal of Solids and Structures* **36** 2091–2108

[23] Colatosti M, Shi F, Fantuzzi N and Trovalusci P 2022 *Materials* **15** 7524

[24] D'Altri A M, Sarhosis V, Milani G, Rots J, Cattari S, Lagomarsino S, Sacco E, Tralli A, Castellazzi G and de Miranda S 2020 *Archives of computational methods in engineering* **27** 1153–1185

[25] 1981 *ASTM 519–81. Standard Test Method for Diagonal Tension (Shear) in Masonry Assemblages* pp 1–17

[26] RILEM TC, 76-LUM 1994 *Recommendations for the Testing and Use of Constructions Materials: Diagonal tensile strength tests of small wall specimens* (RILEM)

[27] De Carvalho Bello C B, Cecchi A, Meroi E and Oliveira D V 2017 Experimental and numerical investigations on the behaviour of masonry walls reinforced with an innovative sisal FRCM system *Key Engineering Materials* vol 747 (Trans Tech Publ) pp 190–195

[28] Borri A, Castori G, Corradi M and Speranzini E 2011 *Construction and Building Materials* **25** 4403–4414

[29] Eberl C 2004 Digital image correlation and tracking MATLAB Central File Exchange URL https://it.mathworks.com/matlabcentral/fileexchange/12413-digital-image-correlation-and-tracking

[30] Cecchi A, Milani G and Tralli A 2005 *Journal of engineering mechanics* **131** 185–198

[31] Sab K and Pradel F 2009 *International journal of computer applications in technology* **34** 60–71

[32] Sulem J and Mühlhaus H B 1997 *Mechanics of Cohesive-frictional Materials: An International Journal on Experiments, Modelling and Computation of Materials and Structures* **2** 31–46

[33] Baraldi D and Cecchi A 2014 Discrete and continuous models for the in plane modal analysis of masonry structures *5th European Conference on Computational Mechanics (ECCM-V)* pp 1–12

[34] Cecchi A and Sab K 2002 *European Journal of Mechanics - A/Solids* **21** 249–268 ISSN 0997-7538

[35] 2007 *BS - EN - 1052-3. Methods of Test for Masonry Part 3: Determination of Initial Shear Strength*

[36] 2011 *BS EN -772-1, Methods of test for masonry units-Part 1: Determination of compressive strength* (European Committee for Standardization, Brussels)

[37] 1999 *BS EN 1015-11: Methods of test for mortar for masonry - Part 11: Determination of flexural and compressive strength of hardened mortar* (European Committee for Standardization, Brussels)